FIRST RESULTS FROM *ATLANTIS*

COLLINEAR LASER SPECTROSCOPY AT ANL

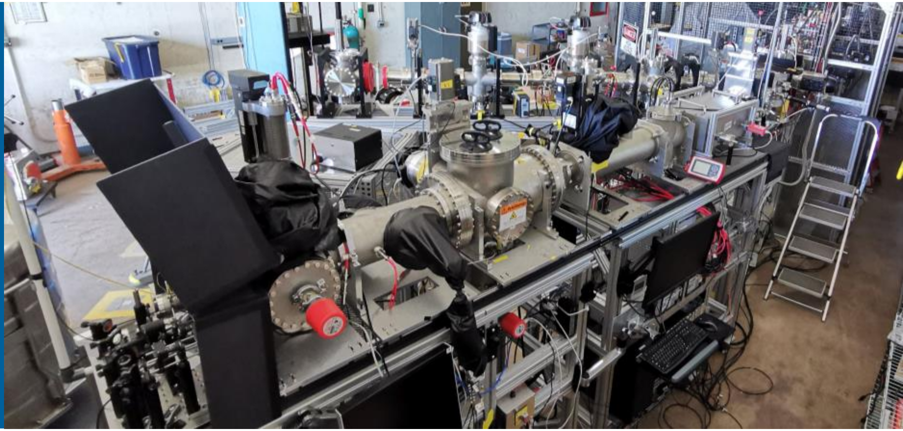

BERNHARD MAASS

TU DARMSTADT, INSTITUT FÜR KERNPHYSIK

ARGONNE NATIONAL LABORATORY

ISOLDE USER WORKSHOP 2023

LASER SPECTROSCOPY

- Atomic levels are influenced by nuclear effects – size, mass, moments
- Precise measurement allows extraction of these observables
- Applicable to short-lived isotopes and isomers

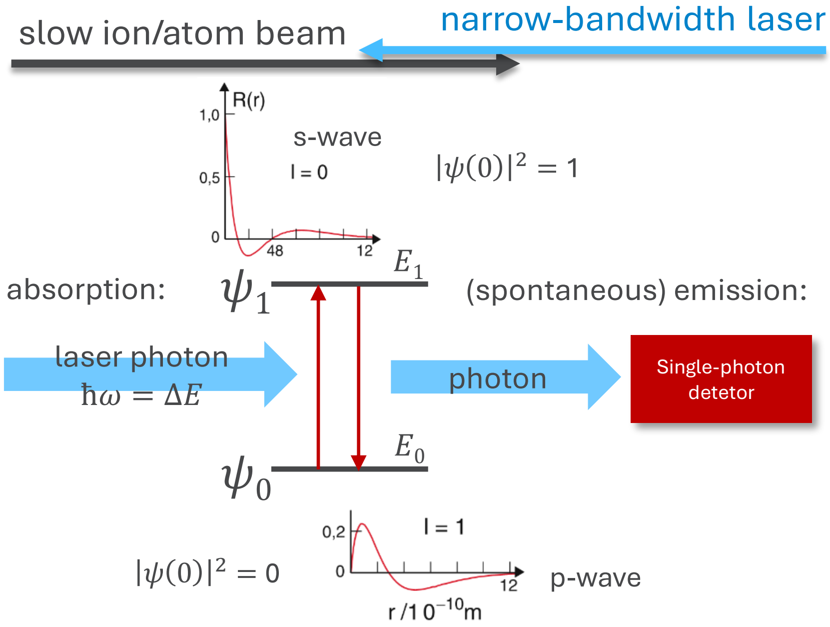

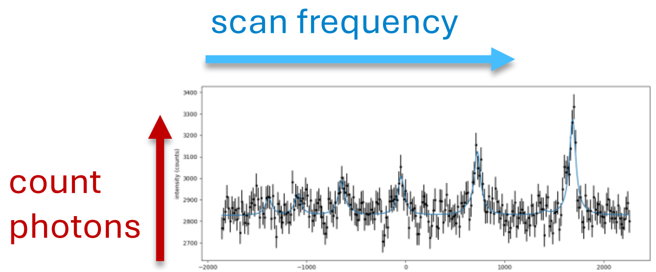

$$\langle r^2 \rangle = \frac{\int_0^\infty \rho(\vec{r})\, r^2 d^3r}{\int_0^\infty \rho(\vec{r})\, d^3r} \qquad \langle r^2 \rangle = \langle r^2 \rangle_0 \left(1 + \frac{5}{4\pi} \sum_{i=2}^{\infty} \langle \beta_i^2 \rangle \right)$$

Accessible observables:

- (difference in) mean-square nuclear charge radii
- Magnetic dipole moment
- Electric quadrupole moment
- Static deformation parameters

LASPEC AT CARIBU

- CARIBU: ^{252}Cf ~~>1C (4x10^{10}Bq)~~ 10mC-spontaneous fission source
- Inside gas catcher to provide slow beams, have been used for mass measurements
- Fission peaks offset from ^{235}U fission – potential for unique beams
- Chemistry of refractory metals is avoided

252Cf
2.645 y

α = 96.91%
SF = 3.09%

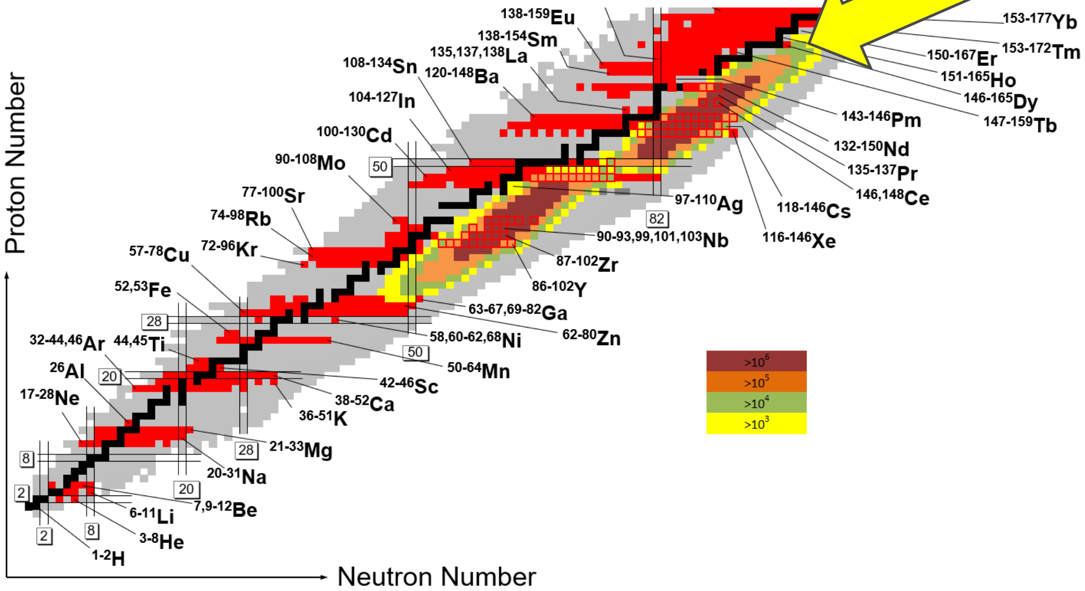

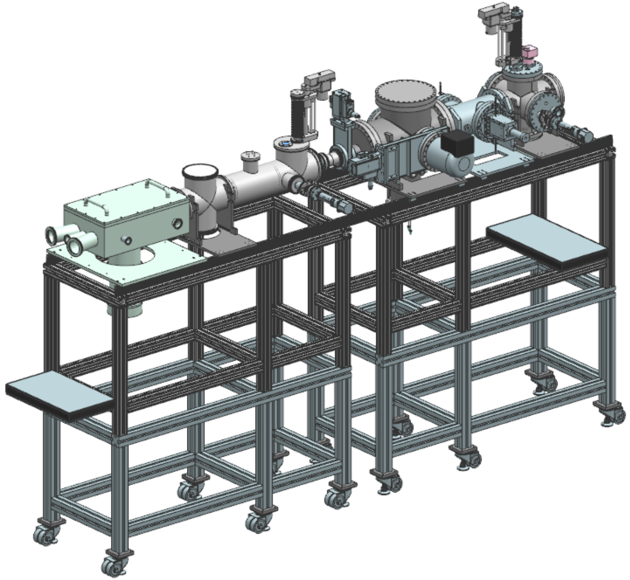

PHYSICS IN THE N=60 REGION

linearity of qp moments in Cd isotopes in the h11/2 orbital

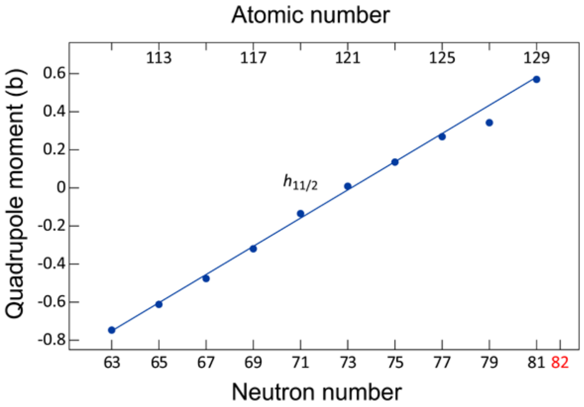

D. T. Yordanov *et al.*, PRL **110**, 192501 (2013)

deformation in mid-shell isotopes across the nuclear chart

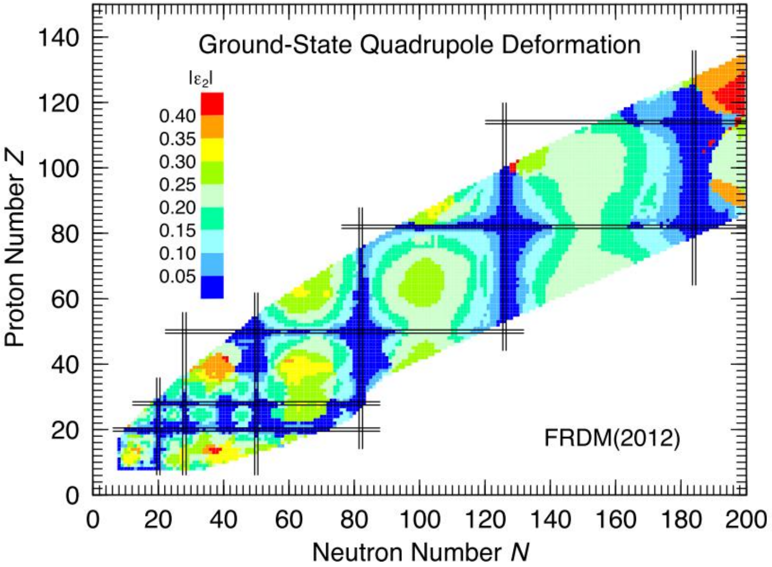

P. Möller, A. J. Sierk, T. Ichikawa, and H. Sagawa, At. Data Nucl. Data Tables **109-110**, 1 (2016)

shape changes and collectivity in N=60 isotopes

F. C. Charlwood *et al.*, Phys. Lett. B **674**, 23 (2009)

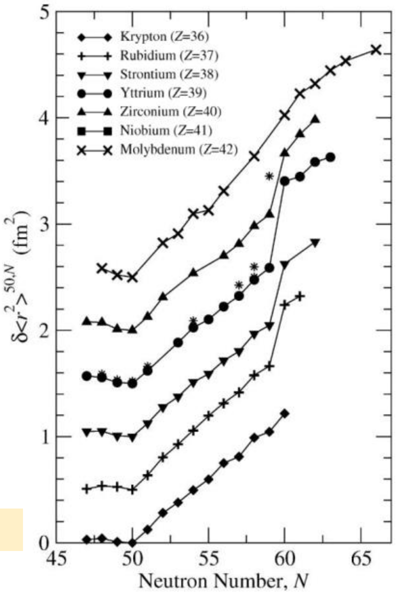

INSTALLATION OF ATLANTIS

- Starting in 2021, we installed:
  - ~10m of transport beamline
  - A new laser ablation source
  - A new cooler/buncher
  - The collinear LS beamline
  - A laser lab

ATL-LAS

- New, reliable pulse laser with ~50mJ, 100Hz, Nd:YAGx2
- Confirmed beams: Pd, Ru, Rh, Gd, Sm, Zr, Ti
- Target swap < 2h beam-beam

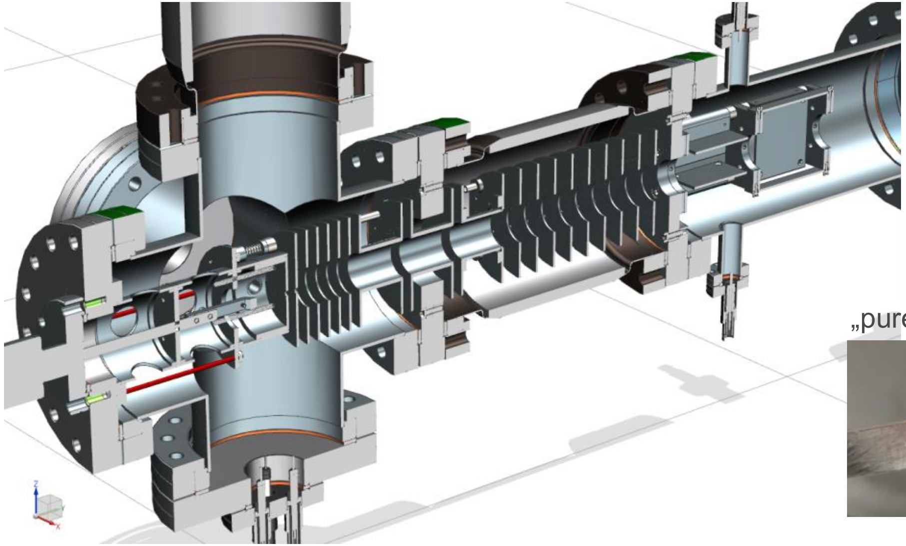

„pure“ targets

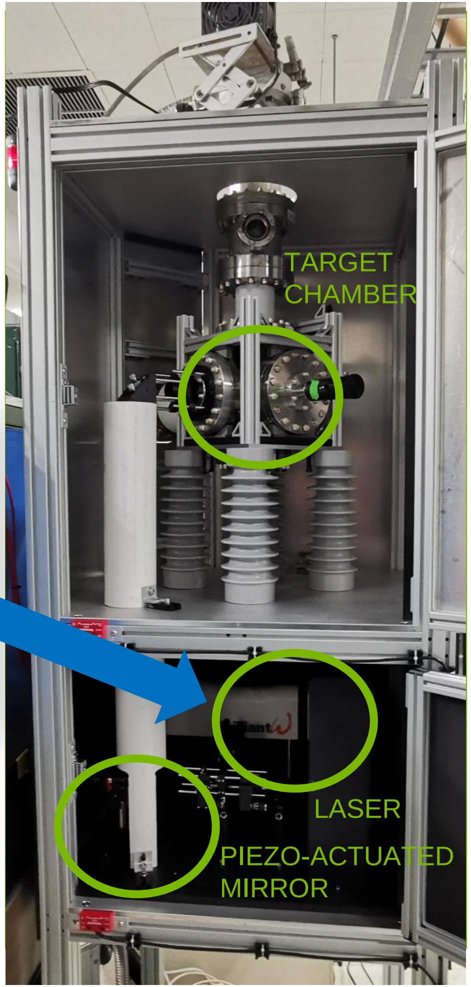

COOLER/BUNCHER

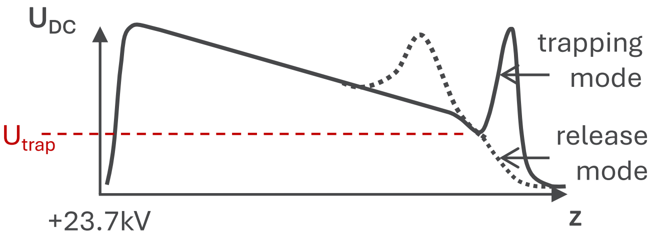

– Bunching compresses the beam into a short time window

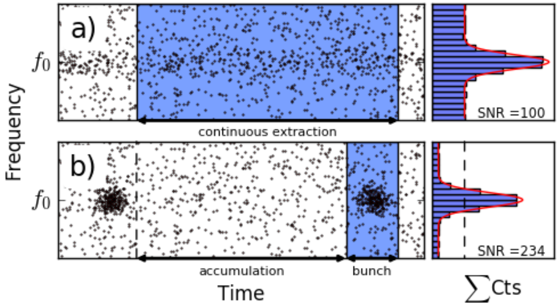

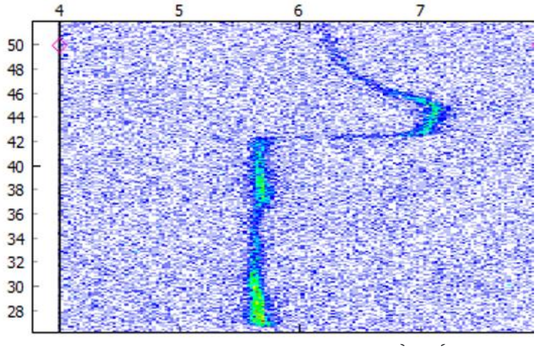

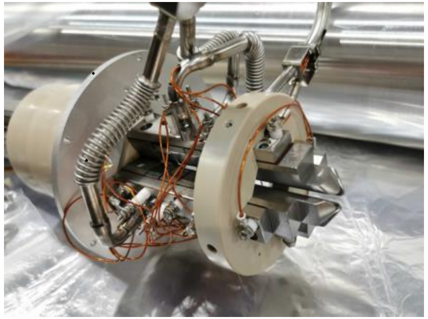

– time focussing:
  - make the bunch as short as possible
– ion stacking
  - collect as many ions as possible in one bunch

COOLER/BUNCHER

– Bunching compresses the beam into a short time window

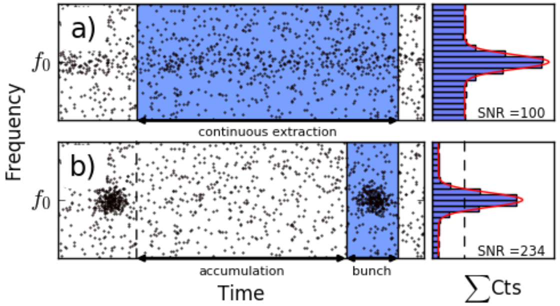

- time focussing:
  - make the bunch as short as possible
- ion stacking
  - collect as many ions as possible in one bunch

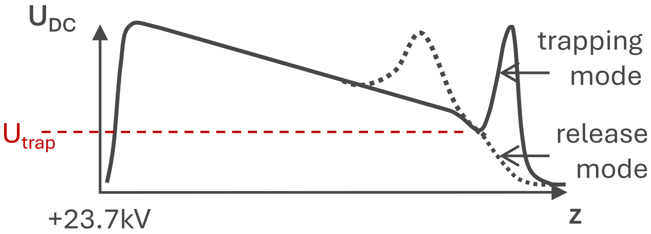

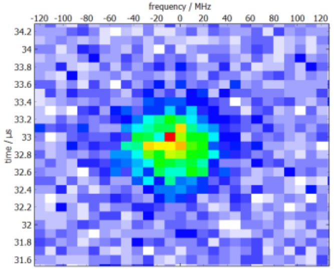

$\Delta t < 1\mu s$

$\Delta E < 40MHz\ (3V)$

eff.: ~80%

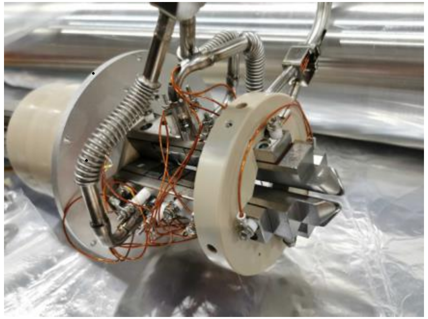

COOLER/BUNCHER

– Bunching compresses the beam into a short time window

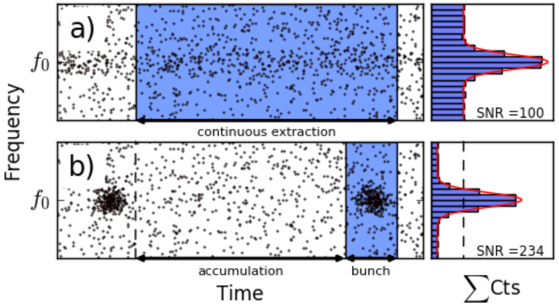

– time focussing:
  - make the bunch as short as possible
– ion stacking
  - collect as many ions as possible in one bunch

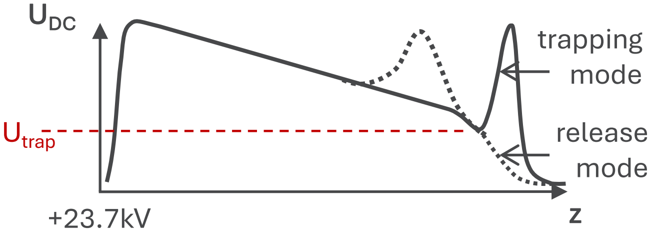

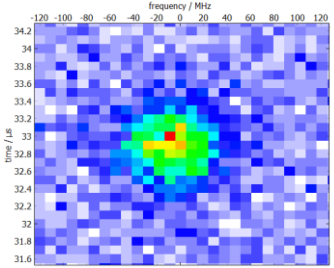

$\Delta t < 1\mu s$

$\Delta E < 40MHz\ (3V)$

eff.: ~80%

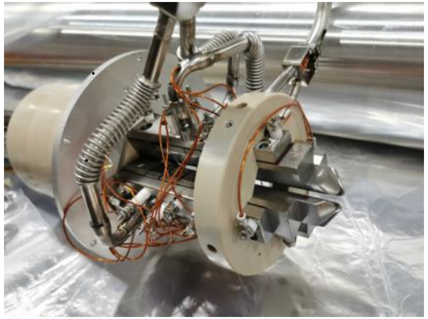

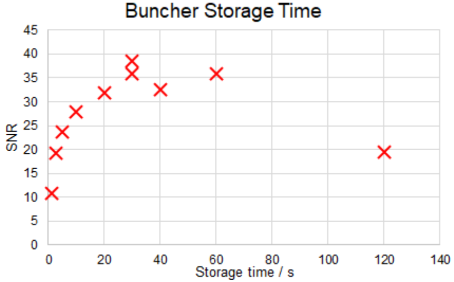

Storage times > 30s

($> t_{1/2}$ for low-rate isotopes)

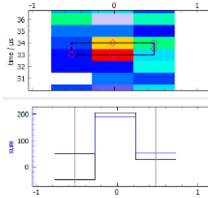

$1{:}10^7$

background suppression (vs. cw)

ATOMIC BEAMS

- upgraded charge-exchange cell developed by Felix Sommer
- optimized for higher temperatures to work with Magnesium
- Near-resonant charge exchange (neutralization) with Ru/Pd ions
- no reflow, small apertures

hot center (~400°C),
filled with Mg – neutralizes beam in-flight

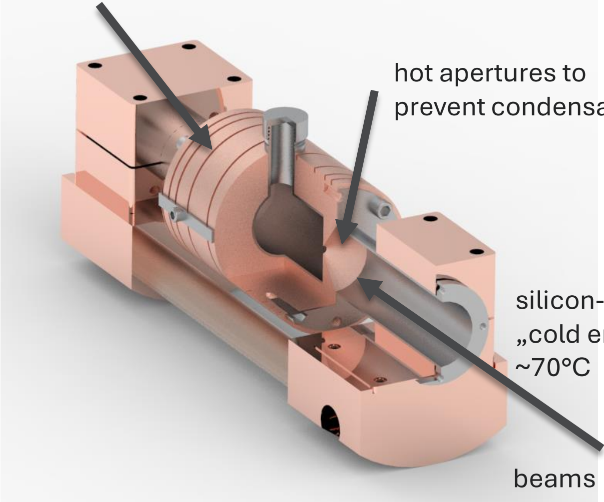

hot apertures to
prevent condensation

silicon-oil cooled
„cold ends“
~70°C

beams
(ions+laser)

360nm

340nm

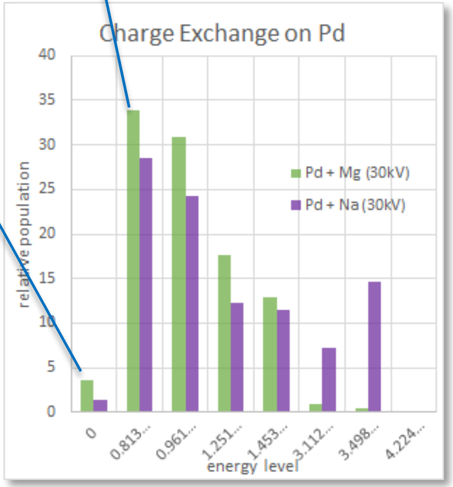

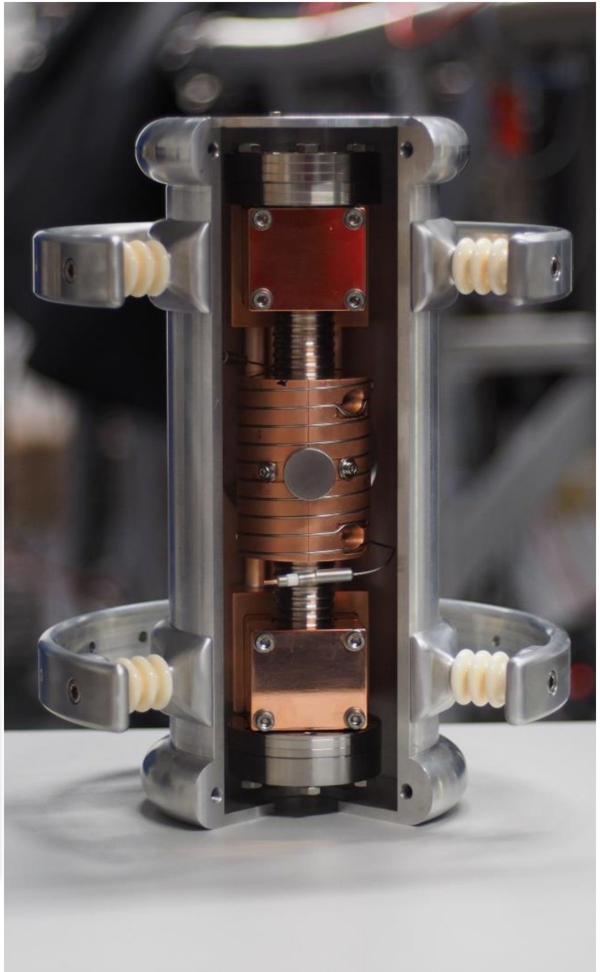

CHARGE EXCHANGE CELL

- one fill (~5g) lasted for 2-3 weeks
- operation at ~360°C – no sidepeaks visible
- efficient g.s. population for Pd & Ru (+Tc, Rh)

Ionization Potential	7.65eV
T (1Pa)	428°C
Melting point	650°C

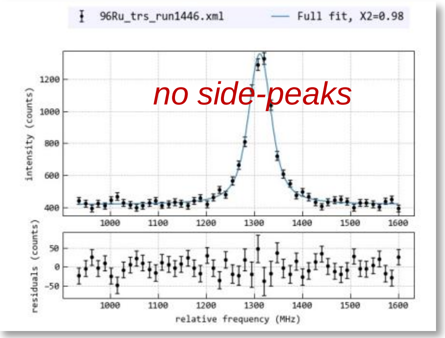

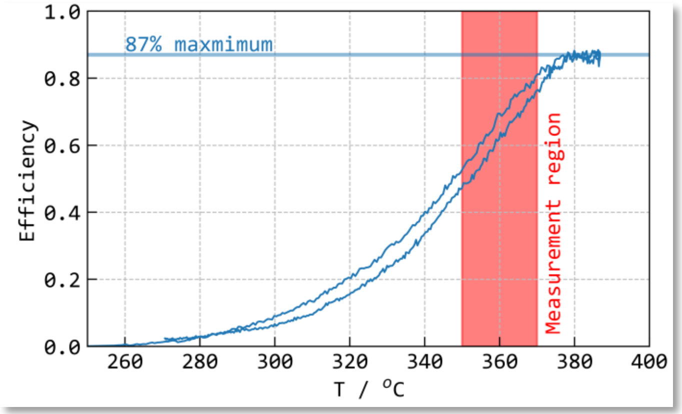

- test the efficiency with simple kicker
- „purify“ beam with long storage time inside the buncher

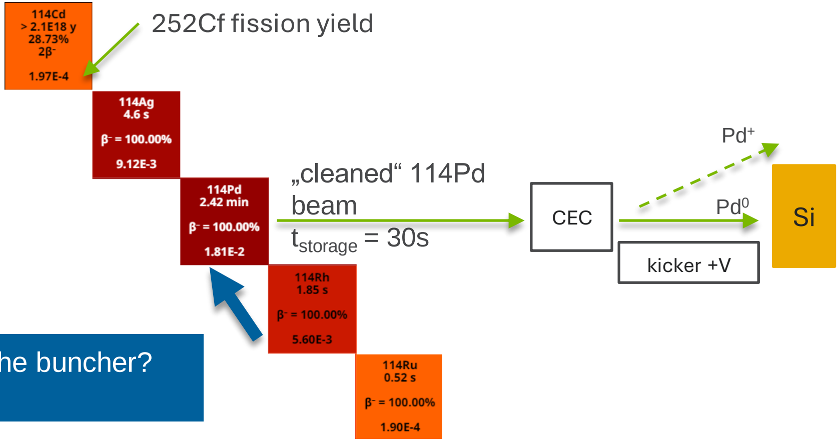

do we store β-decay products in the buncher?
Nuclear Recoil: ~10eV

LASER SPECTROSCOPY AT CARIBU

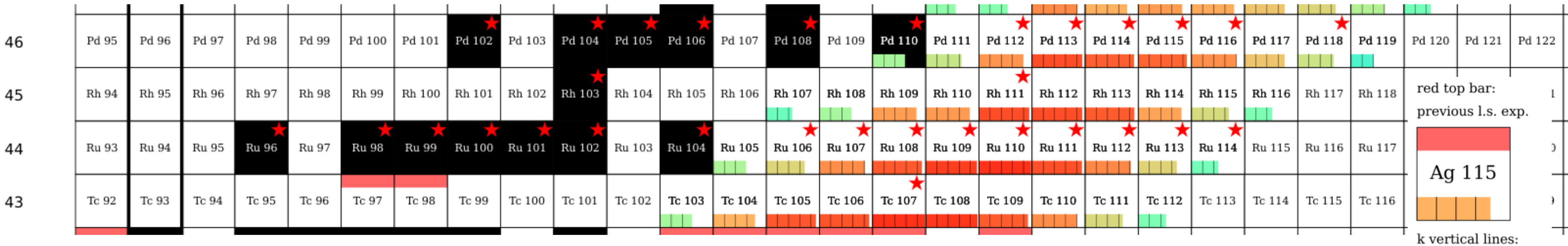

Cf-252 spontaneous fission yield from CARIBU 2022 (x1000)

k vertical lines:
production of 10^k/s
(here: $5.8 \cdot 10^3$)

- Probed over 33 isotopes of 4 different elements in several weeks in November 2022 & March 2023
- many radioactive isotopes that have never been investigated with LS before
- „Complete“ data sets for Ru, complementary Pd data and first hints of Rh & Tc
- Rh, Tc are more difficult due to
  - Lack of stable references
  - Uneven nuclear spin (p uneven)

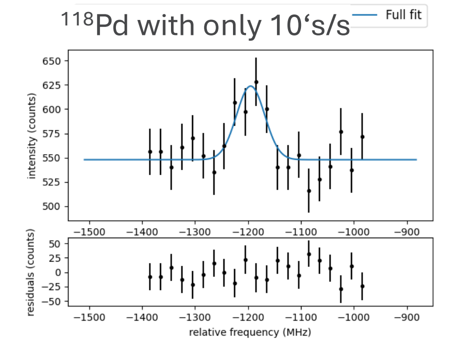

RUTHENIUM

– Measured the optical spectra of 9 neutron-rich Ruthenium isotopes

– More data than presented here
  – search & exclude, statistics, systematics

– Referenced on stable/offline ^{102}Ru
  – Produced in laser ablation ion source
  – Similar beam properties due to bunching

– Confirmed the spin-1/2 assignment for Ru-113

– No isomers were detected
  – adds some ambiguity to some datasets where isomeric half-lives are long

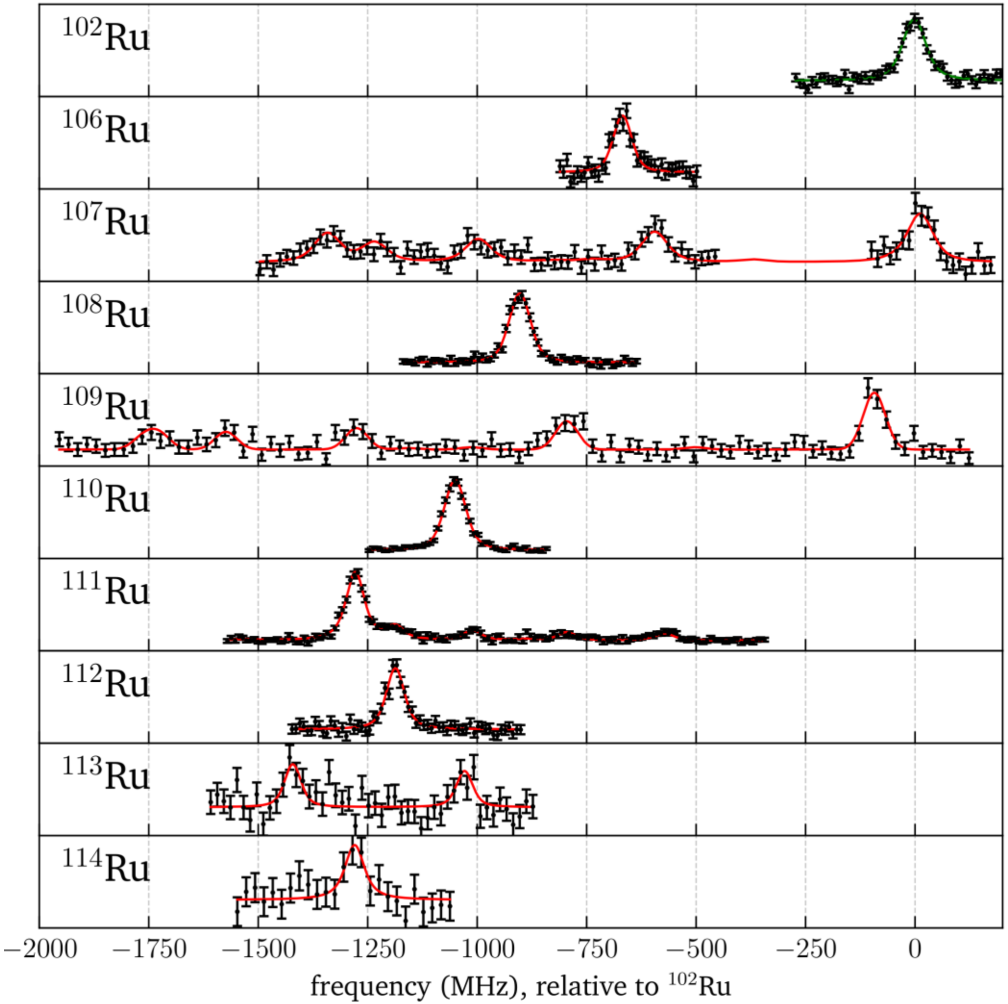

KING PLOT ANALYSIS

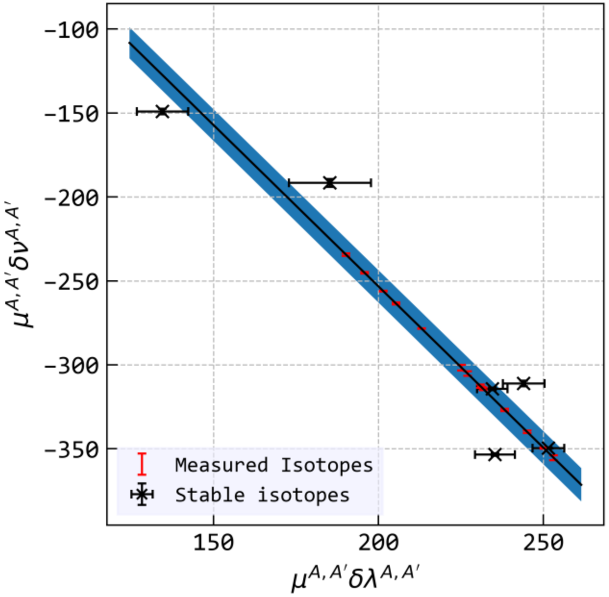

– Isotope shift:

$$\delta\nu_i{}^{A,A'} = \nu_i{}^{A'} - \nu_i{}^{A} = F_i\,\delta\langle r^2\rangle^{A,A'} + M_i\,\frac{m'_A - m_A}{m'_A m_A}$$

– (Re-) measured stable isotopes: 96, 98, 99, 100, 101, 102, 104

– Improved errors by a factor 2-5

– Use known nuclear charge-radii to interpolate the mass and field shift

$$\mu^{A,A'} = \frac{A'\,A}{A' - A}\,\frac{A'_{\mathrm{ref}} - A_{\mathrm{ref}}}{A'_{\mathrm{ref}} A_{\mathrm{ref}}} \qquad \mu^{A,A'}\,\delta\nu_i^{A,A'} = M_i^{A_{\mathrm{ref}},A'_{\mathrm{ref}}} + F_i \mu^{A,A'}\lambda^{A,A'}$$

identifier	IS_val	IS_err	Lit	Literr
104_102	-349.7	0.4	-347	2
100_98	-336.5	1.8	-336	4
98_96	-397.9	0.8	-396	4
102_100	-326.8	0.8	-325	3
99_98	-104.5	1.1	-104	4
101_100	-78.6	0.7	-77	3

D. H. Forest *et al.*, J. Phys. G: Nucl. Part. Phys. **41**, 25106 (2014)

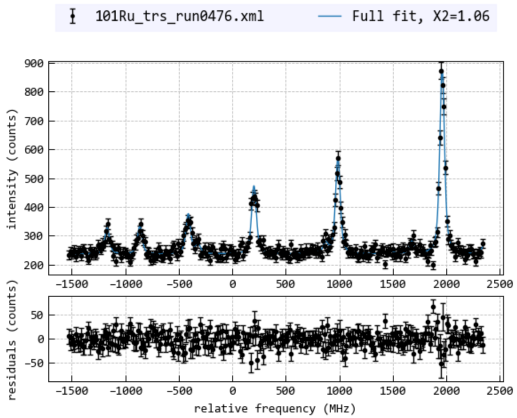

NUCLEAR CHARGE RADII IN THE TIN REGION

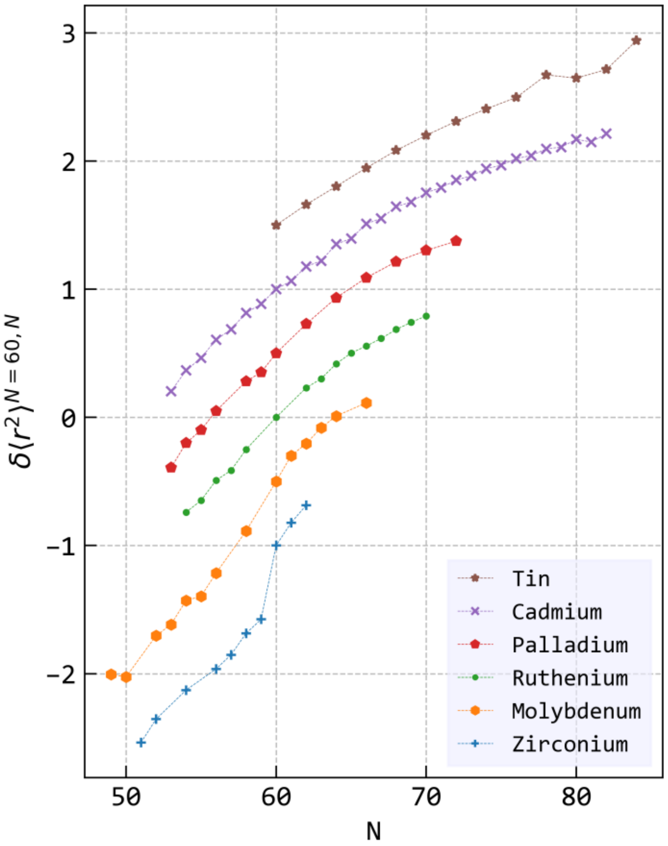

- New measurements in the **Ruthenium** isotopic chain
- Statistical uncertainties negligible. Systematic errors can change the slope.
- Isotopic chains offset by 0.5 fm^2
- Ruthenium: 9 radioactive isotopes measured (106-114)

Sn: F. Le Blanc *et al.*, Phys. Rev. C **72** (2005).
Cd: M. Hammen *et al.*, PRL **121**, 102501 (2018)
Pd: S. Geldhof *et al.*, PRL **128**, 152501 (2022)
Mo: F. C. Charlwood *et al.*, Phys. Lett. B **674**, 23 (2009).
Zr: P. Campbell *et al.*, PRL **89**, 82501 (2002).

NUCLEAR CHARGE RADII OF RUTHENIUM ISOTOPES

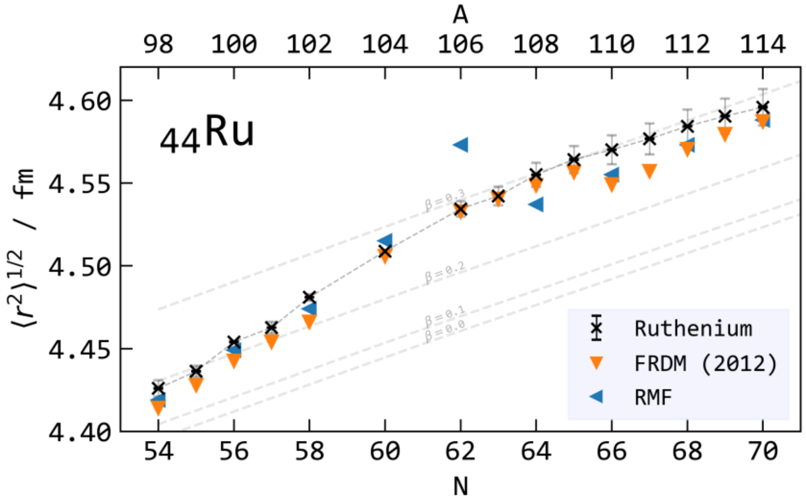

FRDM: P. Möller, A. J. Sierk, T. Ichikawa, and H. Sagawa, At. Data Nucl. Data Tables **109-110**, 1 (2016)
RMF: Lalazissis, G. A., et al., G. A. Lalazissis, S. Raman, and P. Ring, At. Data Nucl. Data Tables **71**, 1 (1999)

S. Geldhof *et al.*, PRL **128**, 152501 (2022)

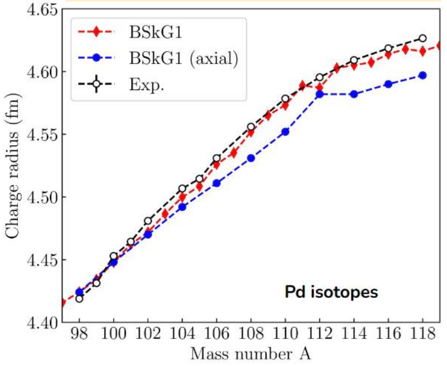

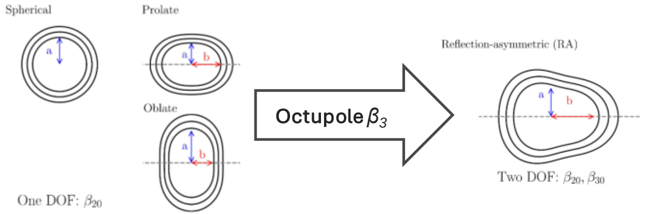

BSkG1: W. Ryssens, G. Scamps, S. Goriely, and M. Bender, Eur. Phys. J. A **58** (2022)

- RMF: Relativistic mean-field calculations
- FRDM: finite-range droplet macroscopic and the folded-Yukawa single-particle microscopic nuclear-structure models

„Skyrme–Hartree–Fock–Bogoliubov mass models on a 3D mesh“ (triaxial, reflection-asymmetric)

NUCLEAR CHARGE RADII OF RUTHENIUM ISOTOPES

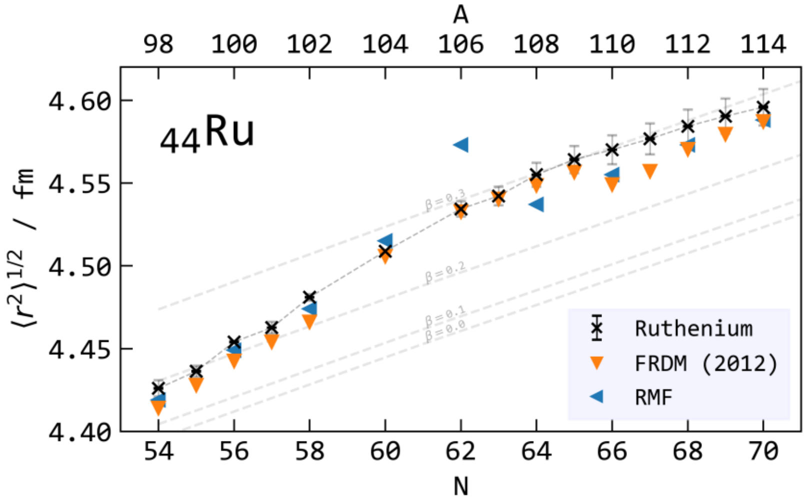

FRDM: P. Möller, A. J. Sierk, T. Ichikawa, and H. Sagawa, At. Data Nucl. Data Tables **109-110**, 1 (2016)
RMF: Lalazissis, G. A., et al., G. A. Lalazissis, S. Raman, and P. Ring, At. Data Nucl. Data Tables **71**, 1 (1999)

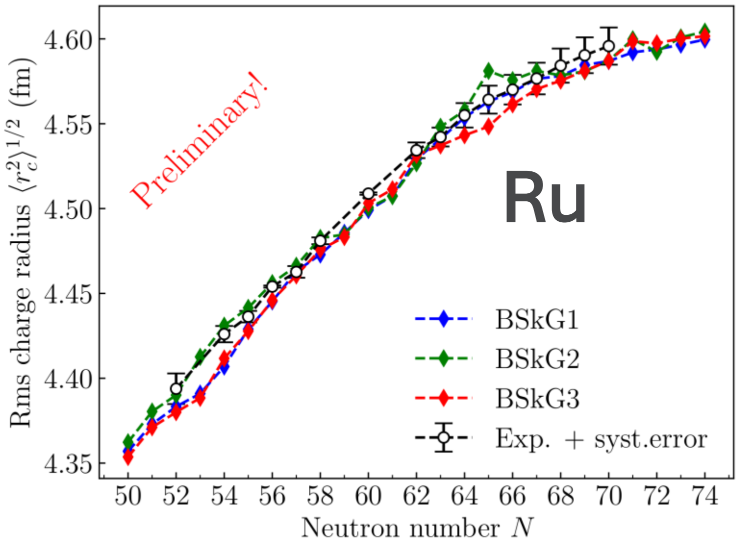

- RMF: Relativistic mean-field calculations
- FRDM: finite-range droplet macroscopic and the folded-Yukawa single-particle microscopic nuclear-structure models

BSkG1: W. Ryssens, G. Scamps, S. Goriely, and M. Bender, Eur. Phys. J. A **58** (2022)

„Skyrme–Hartree–Fock–Bogoliubov mass models on a 3D mesh“ (triaxial, reflection-asymmetric)

STATIC QUADRUPOLE? DEFORMATION

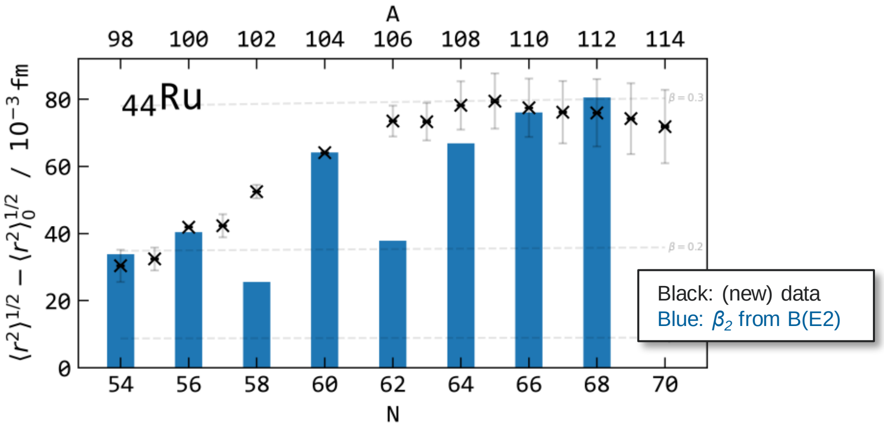

– LS mean-square nuclear charge radii are sensitive to the r^2-long-range part of the nuclear wave function

$$\langle r^2\rangle = \frac{\int_0^\infty \rho(\vec{r})\, r^2 d^3r}{\int_0^\infty \rho(\vec{r})\, d^3r}$$

– This includes nuclear deformation parameters β_i

$$\langle r^2\rangle = \langle r^2\rangle_0 \left(1 + \frac{5}{4\pi}\sum_{i=2}^{\infty}\langle\beta_i^2\rangle\right)$$

– Extract β_2 from nuclear spectroscopy B(E2) strength and plot difference to spherical Liquid drop model (LDM)

– Can β_2 explain the full LDM deviation?

$$\beta_2 = \frac{4\pi}{3zR_0^2}\left[\frac{B(E2)\uparrow}{e^2}\right]^{1/2}$$

Change from prolate to oblate deformation calculated with HFB method, Gogny functional D1M

K. Nomura, R. Rodríguez-Guzmán, and L. M. Robledo, PRC **94** (2016).

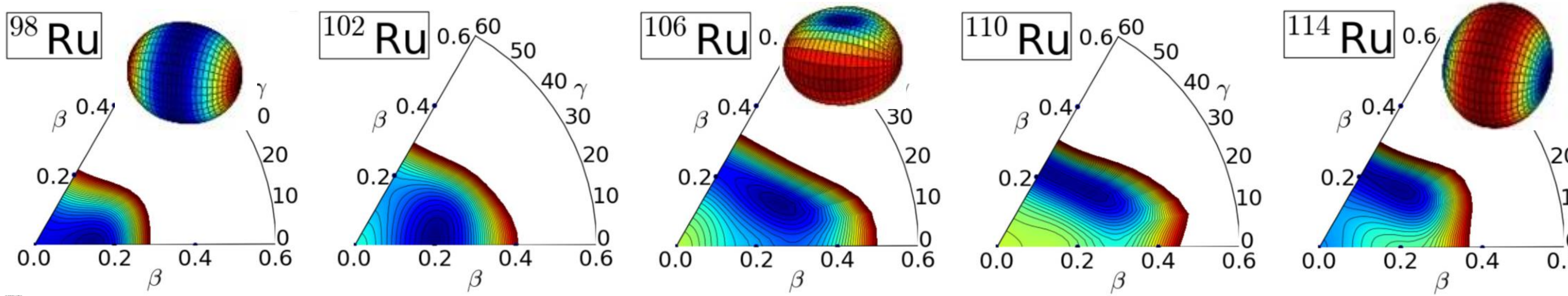

FUTURE AT (NU)CARIBU

- Upgrading CARIBU to neutron induced ^{235}U (and other actinides) fission
- Protons from 7MeV tandem → ^{7}Li converter target
- Neutron moderator to 2.3MeV fission cross section maximum

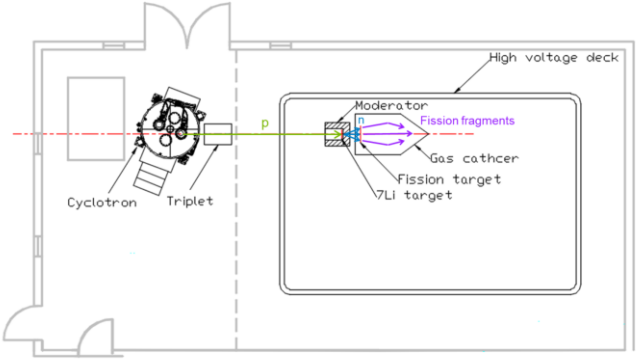

- PAC-approved proposals for:
  - Cer/Neodymium (inversion of β_2-values beyond N=90)
  - Technetium (NCR of radioactive Tc isotopes)
- Lanthanum 2+ (by FRIB / BECOLA group, K. Minamisono)
- collinear measurement of $^{10,11}B$

B. Cheal *et al.*, J. Phys. G: Nucl. Part. Phys. **29**, 2479 (2003)

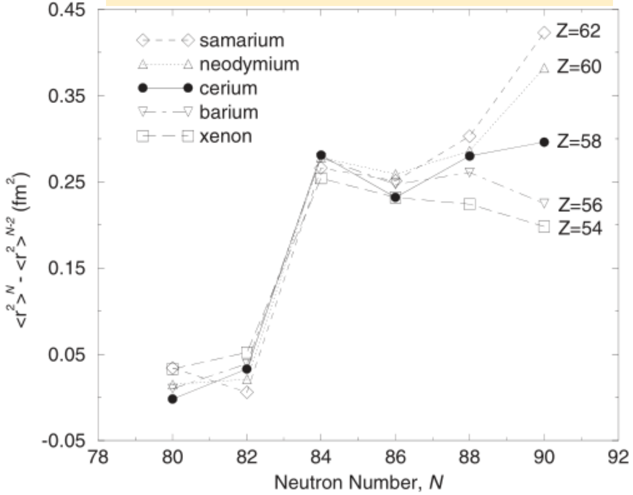

$$\delta\langle r^2\rangle = \delta\langle r^2\rangle_{\text{sph}} + \langle r^2\rangle_{\text{sph}}\frac{5}{4\pi}\sum_i \delta\langle\beta_i^2\rangle$$

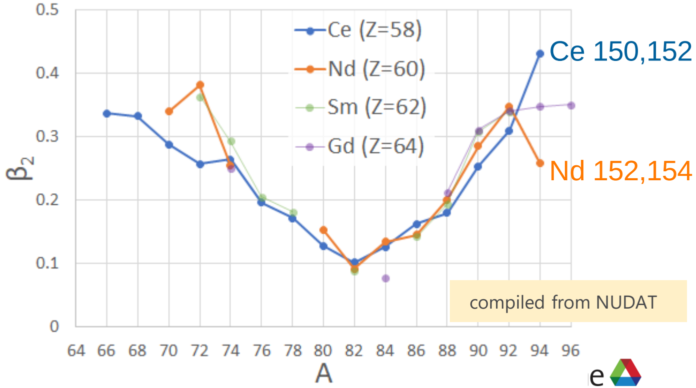

ATLANTIS - ARGONNE TANDEM HALL LASER BEAMLINE FOR ATOM AND ION SPECTROSCOPY

Bernhard Maass[1], Alex Brinson[2,3], Daniel Burdette[1], Jason Clark[1], Adam Dockery[3], Max Horst[4,5], Phillip Imgram[4], Kristian König[4], Kei Minamisono[3], Patrick Müller[4], Peter Müller[1], Wilfried Nörtershäuser[4,5], Skyy Pineda[3], Simon Rausch[4,5], Laura Renth[4], Brooke Rickey[3], Daniel Santiago-Gonzalez[1], Guy Savard[1], Felix Sommer[4], Adrian Valverde[1,6]

[1]Physics Division, Argonne National Laboratory, Lemont, IL 60439, USA

[2]Massachusetts Institute of Technology, Cambridge, MA, USA

[3]Facility for Rare Isotope Beams, Michigan State University, East Lansing 48824, USA

[4]Institut für Kernphysik, Technische Universität Darmstadt, 64289 Darmstadt, Germany

[5]Helmholtz Forschungsakademie Hessen für FAIR, Darmstadt, Germany

This work was supported by **DFG – Project-Id 279384907-SFB 1245**, **BMBF 05P19RDFN1** and **NSF Grant No. PHY-21-11185**, and by the **U.S. Department of Energy, Office of Nuclear Physics**, under **Contract No. DE-AC02-06CH11357**, with resources of **ANL's ATLAS facility**, an Office of Science User Facility.

THANK YOU FOR YOUR ATTENTION!

N=126

- New low-energy experimental area at ANL
- target/gas catcher combination behind ATLAS accelerator
- uses the cooler/buncher design from CARIBU
- copy of ATL-LAS is being built
- in early commissioning phase

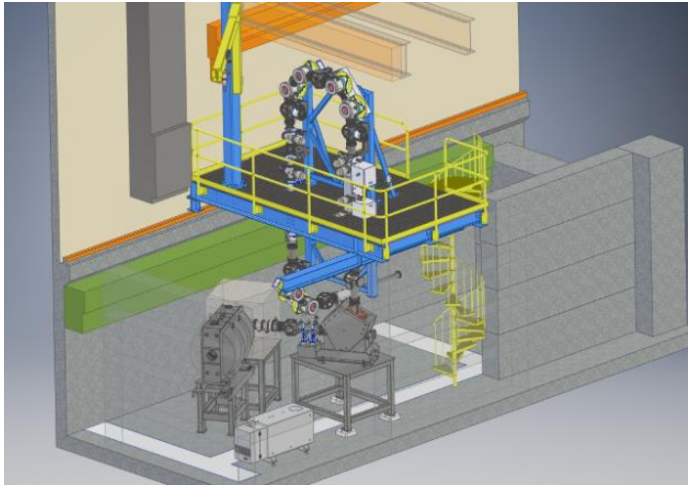

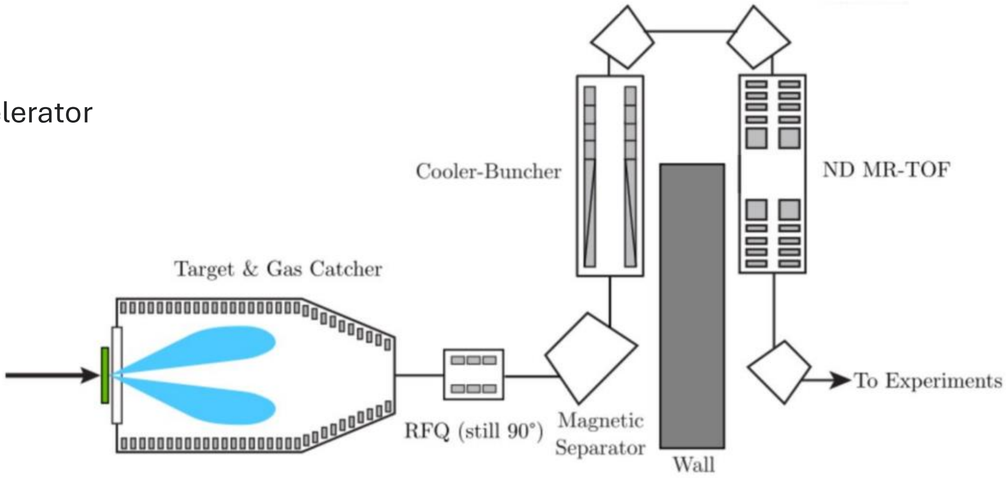

<u>key experiments</u>

- decay station (X-Array)
- mass measurements (CPT)
- laser spectroscopy

N=126

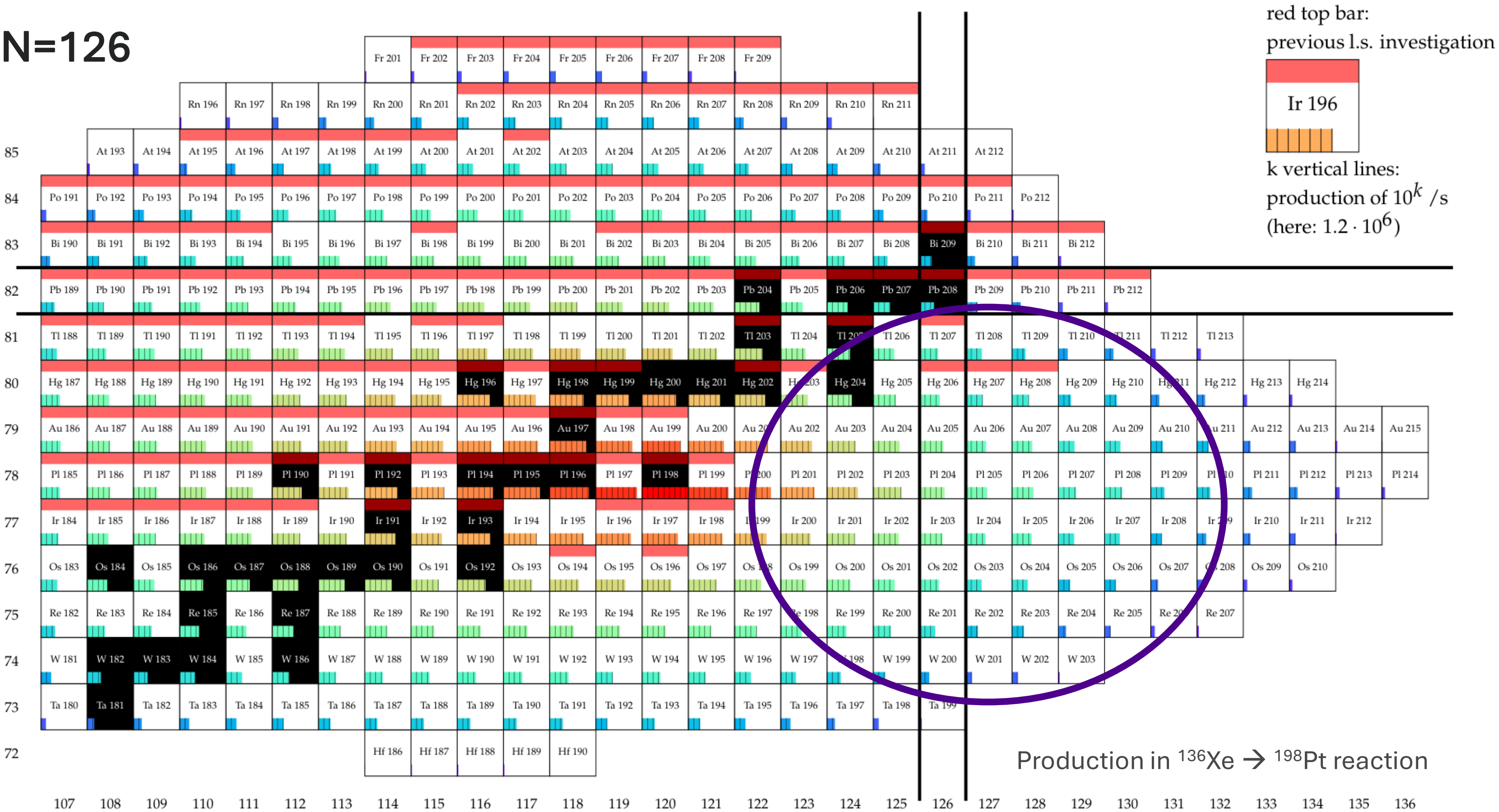
red top bar:
previous l.s. investigation
Ir 196
k vertical lines:
production of 10^k /s
(here: $1.2 \cdot 10^6$)
Fr 201 Fr 202 Fr 203 Fr 204 Fr 205 Fr 206 Fr 207 Fr 208 Fr 209
Rn 196 Rn 197 Rn 198 Rn 199 Rn 200 Rn 201 Rn 202 Rn 203 Rn 204 Rn 205 Rn 206 Rn 207 Rn 208 Rn 209 Rn 210 Rn 211
85 At 193 At 194 At 195 At 196 At 197 At 198 At 199 At 200 At 201 At 202 At 203 At 204 At 205 At 206 At 207 At 208 At 209 At 210 At 211 At 212
84 Po 191 Po 192 Po 193 Po 194 Po 195 Po 196 Po 197 Po 198 Po 199 Po 200 Po 201 Po 202 Po 203 Po 204 Po 205 Po 206 Po 207 Po 208 Po 209 Po 210 Po 211 Po 212
83 Bi 190 Bi 191 Bi 192 Bi 193 Bi 194 Bi 195 Bi 196 Bi 197 Bi 198 Bi 199 Bi 200 Bi 201 Bi 202 Bi 203 Bi 204 Bi 205 Bi 206 Bi 207 Bi 208 Bi 209 Bi 210 Bi 211 Bi 212
82 Pb 189 Pb 190 Pb 191 Pb 192 Pb 193 Pb 194 Pb 195 Pb 196 Pb 197 Pb 198 Pb 199 Pb 200 Pb 201 Pb 202 Pb 203 Pb 204 Pb 205 Pb 206 Pb 207 Pb 208 Pb 209 Pb 210 Pb 211 Pb 212
81 Tl 188 Tl 189 Tl 190 Tl 191 Tl 192 Tl 193 Tl 194 Tl 195 Tl 196 Tl 197 Tl 198 Tl 199 Tl 200 Tl 201 Tl 202 Tl 203 Tl 204 Tl 206 Tl 207 Tl 208 Tl 209 Tl 210 Tl 212 Tl 213
80 Hg 187 Hg 188 Hg 189 Hg 190 Hg 191 Hg 192 Hg 193 Hg 194 Hg 195 Hg 196 Hg 197 Hg 198 Hg 199 Hg 200 Hg 201 Hg 202 Hg 204 Hg 205 Hg 206 Hg 207 Hg 208 Hg 209 Hg 210 Hg 212 Hg 213 Hg 214
79 Au 186 Au 187 Au 188 Au 189 Au 190 Au 191 Au 192 Au 193 Au 194 Au 195 Au 196 Au 197 Au 198 Au 199 Au 200 Au 202 Au 203 Au 204 Au 205 Au 206 Au 207 Au 208 Au 209 Au 210 Au 212 Au 213 Au 214 Au 215
78 Pt 185 Pt 186 Pt 187 Pt 188 Pt 189 Pt 190 Pt 191 Pt 192 Pt 193 Pt 194 Pt 195 Pt 196 Pt 197 Pt 198 Pt 199 Pt 201 Pt 202 Pt 203 Pt 204 Pt 205 Pt 206 Pt 207 Pt 208 Pt 209 Pt 211 Pt 212 Pt 213 Pt 214
77 Ir 184 Ir 185 Ir 186 Ir 187 Ir 188 Ir 189 Ir 190 Ir 191 Ir 192 Ir 193 Ir 194 Ir 195 Ir 196 Ir 197 Ir 198 Ir 200 Ir 201 Ir 202 Ir 203 Ir 204 Ir 205 Ir 206 Ir 207 Ir 208 Ir 210 Ir 211 Ir 212
76 Os 183 Os 184 Os 185 Os 186 Os 187 Os 188 Os 189 Os 190 Os 191 Os 192 Os 193 Os 194 Os 195 Os 196 Os 197 Os 199 Os 200 Os 201 Os 202 Os 203 Os 204 Os 205 Os 206 Os 207 Os 209 Os 210
75 Re 182 Re 183 Re 184 Re 185 Re 186 Re 187 Re 188 Re 189 Re 190 Re 191 Re 192 Re 193 Re 194 Re 195 Re 196 Re 197 Re 199 Re 200 Re 201 Re 202 Re 203 Re 204 Re 205 Re 207
74 W 181 W 182 W 183 W 184 W 185 W 186 W 187 W 188 W 189 W 190 W 191 W 192 W 193 W 194 W 195 W 196 W 197 W 199 W 200 W 201 W 202 W 203
73 Ta 180 Ta 181 Ta 182 Ta 183 Ta 184 Ta 185 Ta 186 Ta 187 Ta 188 Ta 189 Ta 190 Ta 191 Ta 192 Ta 193 Ta 194 Ta 195 Ta 196 Ta 197 Ta 198 Ta 199
72 Hf 186 Hf 187 Hf 188 Hf 189 Hf 190
107 108 109 110 111 112 113 114 115 116 117 118 119 120 121 122 123 124 125 126 127 128 129 130 131 132 133 134 135 136
Production in $^{136}Xe \rightarrow {}^{198}Pt$ reaction

LASER SPECTROSCOPY

– probing the electromagnetic interaction of electrons and nuclei
– bound-state electrons provide a non-destructive method to probe the nuclear volume

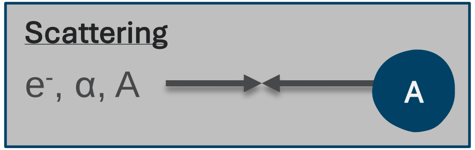

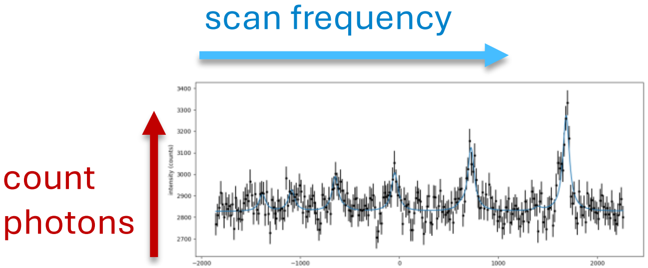

p orbital

$|\psi(0)|^2 = 0$

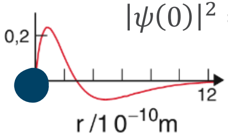

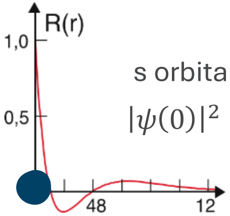

s orbital

$|\psi(0)|^2 > 0$

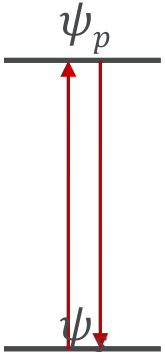

$$\langle r^2 \rangle = \frac{\int_0^\infty \rho(\vec{r})\, r^2 d^3 r}{\int_0^\infty \rho(\vec{r})\, d^3 r}$$

$$\langle r^2 \rangle = \langle r^2 \rangle_0 \left(1 + \frac{5}{4\pi} \sum_{i=2}^{\infty} \langle \beta_i^2 \rangle \right)$$

(spontaneous) emission:

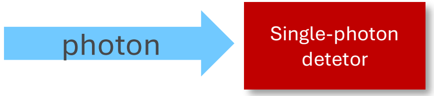

absorption:

p-wave

Accessible observables:

- (difference in) mean-square nuclear charge radii
- Magnetic dipole moment
- Electric quadrupole moment
- Static deformation parameters